2014

# Janus Devices for Gastrointestinal Drug Delivery

Young-Ah Lee
ylee6@wellesley.edu

# JANUS DEVICES FOR GASTROINTESTINAL DRUG DELIVERY

Young-Ah (Lucy) Lee

Advisors: Dr. Nolan T. Flynn, Wellesley College Chemistry

Dr. Robert S. Langer & Dr. C. Giovanni Traverso, MIT Chemical Engineering

Submitted in partial fulfillment of the requirements for

Bachelor of Arts Degree with Honors in Chemistry

at Wellesley College

May 2014

# *Abstract*

As medication compliance presents a key challenge for patients, there is a significant need for enabling longer retention of drug-delivery vehicles to provide extended drug release. This project aims to develop a drug-delivery device with the unique capacity for extended gastrointestinal (GI) retention and drug release. The goal is accomplished by fabricating a novel Janus device with an omniphobic (repellent to everything) side and a mucosal adhesive side. This dual-layer system enables repulsion of the food stream by the omniphobic side and allows attachment to the wall of the GI tract with the mucoadhesive side. The omniphobic side was created using an adapted version of the Slippery Liquid-Infused Porous Surface (SLIPS) system. The fabrication procedure involved biomimetic morphological replication of the nano-structures present on natural lotus leaves using soft lithography, followed by chemical surface modification through fluorination and lubrication. Two different approaches were used to achieve mucoadhesion: first, the application of mussel-inspired surface chemistry to create an adherent polydopamine coating and second, the use of Carbopol, a well-accepted mucoadhesive polymer. The morphology of the omniphobic side was visualized with scanning electron microscopy. Omniphobicity and mucoadhesion of each side were characterized using static contact angle goniometry with various liquids. The protocol for creating the desired Janus device was designed and carried out successfully. *In vitro* studies using porcine tissues demonstrated that the dual-sided Janus device enabled extended retention on the GI mucosal surface. Studies using rat models are planned to assess extended retention and drug release *in vivo*. With successful fabrication and validation, this engineered Janus device will have promising biomedical applications with the potential to improve treatment for various diseases.

# *Acknowledgments*

I would not have been able to survive the completion of this honors senior thesis without help. Therefore, I would like to extend my heartfelt thanks to the following people:

First and foremost, I would like to express my utmost gratitude to all my thesis mentors, **Nolan Flynn, Giovanni Traverso, Robert Langer,** and **Shiyi Zhang**. Nolan, thank you for your infinite support over the four years of my Wellesley career. I feel extremely fortunate to have found you as my mentor and truly appreciate your encouragement, unending patience, and of course, your witty humor. Your guidance and teaching throughout the years have been invaluable to me. Thank you, Gio and Shiyi, for introducing me to the worlds of GI and of polymer science. You have given me a wonderful opportunity to explore research outside of Wellesley. I really appreciate your endless guidance and continual support. Thank you, Dr. Langer, for providing me with the facilities and resources to carry out this project from its inception.

I would also like to thank **Carla Verschoor**, **Don Elmore**, and **Sun-Hee Lee** for agreeing to serve on my thesis committee. Thank you for your insightful questions, input, and advice. I would like to extend my gratitude to all of the faculty members in the Wellesley College Chemistry Department for sharing their love and enthusiasm for chemistry with us.

To all of the GI Team members at the MIT Langer Lab, past and present, thank you for being supportive! To all my friends and especially to my team of moral support at Wellesley, **Farrah Yhee, Maria Jun, Janet Jeong,** and **Anastasia Hou**, thank you for being the best group of friends I could have ever asked for. You kept me sane and made my experience at Wellesley so enjoyable and memorable. I feel incredibly fortunate to know such amazing people!

I would also like to acknowledge Wellesley College, MIT, and my sources of funding - the Jerome A. Schiff Fellowship and the Bill and Melinda Gates Foundation - for supporting this research.

Finally, I would like to thank my amazing family, **Dad, Mom**, and **Sis.** Thank you for being my most loyal and dependable supporters. Thank you for sticking by me through the best and worst moments of my life. I love you all so much!

Thank you.

# *Table of Contents*

# 1. INTRODUCTION

## 1.1 The Unmet Need – Medication Compliance

It is hard being a patient, specifically taking medications on time and at the prescribed doses. As Dr. C. Everett Koop said, "Drugs don't work in patients who don't take them."[1] Poor compliance to treatment of chronic illnesses is a critical public health problem.[2] For example, one study reported a 97% compliance rate at the beginning of treatment with statins, which are drugs used to lower cholesterol levels, but only about 50% of patients were still compliant after six months.[3] The World Health Organization noted that compliance to long-term therapy for chronic diseases in developed countries averages 50%; the rates of compliance are even lower in developing countries.[2] Medication compliance poses a major challenge to patients, yet it is a key aspect of effective clinical care for infectious diseases. Thus, promoting compliance to existing therapies may be the best investment for tackling chronic conditions and the most efficient method of improving health of the population.[1]

The oral route remains the favored route of delivering drugs to patients.[4,5] A series of attractive advantages support this fact, including ease of administration, flexibility on dosing, and avoidance of pain and discomfort usually associated with injections.[4,5] Hence, much attention is concentrated on oral medication compliance. One approach to promote medication compliance for oral delivery is to extend gastrointestinal (GI) retention of the drug delivery system, thereby reducing the frequency of drug administration. Indeed, GI retention is targeted because the duration of oral drug release is predominantly limited by the fast GI transit times of oral dosage forms, which range from 6 to 8 hours in healthy humans.[6,7]

Our goal is to develop a drug-delivery vehicle that has the unique capacity for extended GI retention. In order to achieve extended release of orally administered drugs, strong GI mucosal adhesion of the drug-carrying vehicle is needed. However, this goal is challenging to achieve because adhesion to the GI wall is significantly hindered by the constant passage of foodstuffs and bodily fluids. Hence, the drug delivery system should be designed to minimize the interaction with foodstuffs and reduce the likelihood of dislodgement. We hypothesized that a dual-sided device, called a Janus device, with an omniphobic (repellent to everything) side and a mucosal adhesive side could enable repulsion of the food stream and allow attachment to the wall of the GI tract, respectively. We propose *a facile approach to develop a novel drug-delivery device that would avoid easy detachment by and aggregation with foodstuffs in the GI tract.*

### 1.2 Janus Devices

Janus devices, initially named after the double-faced Roman god Janus, have different properties at opposite sides, comprising two or more components of different chemistries,

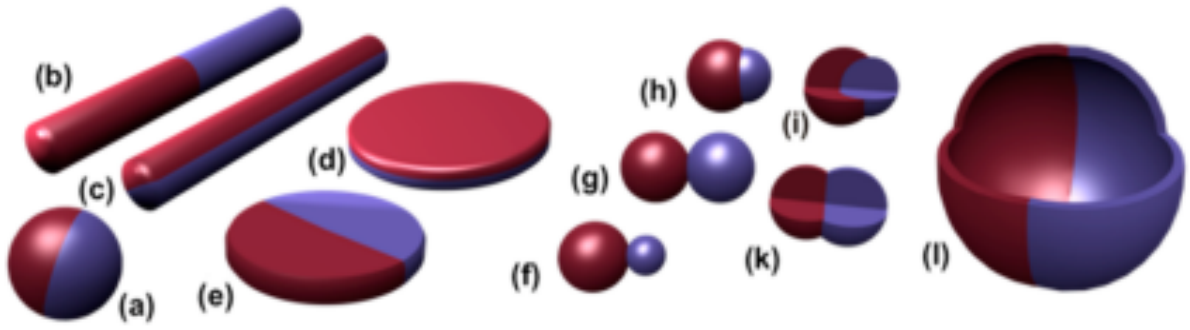


**Figure 1-1.** Janus devices at various sizes and shapes for different applications. Adapted from Walther and Müller.[8]

functionalities, and characteristics.[8] Figure 1-1 shows several different geometries for Janus devices with each face possessing a different color.[8] The term "Janus" was originally coined

by Casagrande and Veyssié in 1988 when they released the first publication about Janus devices; they made glass spherical particles with one hemisphere hydrophilic and the other one hydrophobic.[9] Then, Pierre-Gilles de Gennes, 1991 Nobel Prize winner in physics, publicly reiterated the concept to the scientific community in his "Soft Matter" Nobel Laureate speech.[10] Since then, especially in the past decade, Janus particles have gained much attention in a wide range of applications (*e.g.* in magnetics, plasmonics, colloidal chemistry, optics, and particularly, biomedicine); this is because of their capacity to have multiple functionalities and properties (optical activity, mechanical strength, magnetism, conductivity, *etc*.) within a single particle.[11] In the case of drug delivery applications, Hwang *et al*. developed Janus particles with different biodegradable polymer compartments by using electrohydrodynamic cojetting processes, followed by controlled cross-linking.[12] These Janus particles were composed of an interpenetrating polymer network of poly(ethylene oxide) and polyacrylamide/poly(acrylic acid) (PAAm-*co*-AA) in one hemisphere and a chemically cross-linked copolymer of dextran and PAAm-*co*-AA segments in the other compartment. These particles were expected to find use for orally administrated drugs, as different compartments released their cargo at different physiological pH, giving a complex release profile.

Another biomedical use includes diagnostic applications, where Janus nanoparticles show potential use as probes. For example, inorganic heterodimer nanoparticles of FePt-Au with polyethylene glycol based ligands functionalized on their surfaces were tested as probes for magnetic resonance imaging (MRI) of tumor cell targets.[13] The heterodimers of FePt-Au were conjugated with HmenB1 antibodies, which specifically recognized polysialic acid in tumor cells. In addition to MRI imaging, these hybrid nanoparticles had other innate

multimodal capabilities for biological detection, including catalytic growth effects and optical signal enhancing properties.

Moreover, Janus nanoparticles with optical and magnetic properties can be applied for high potential diagnostic and therapeutic uses. For example, the spherical Janus nanocomposites of magnetic nanoparticles/pyrene-labeled poly-(styrene-block-allyl alcohol) were fabricated to image and treat cancer cells.[14] These nanostructures had spatially separated functionalities for combined fluorescence imaging and magnetolytic therapy of cancer cells. Different from these previous studies, our project proposes an unprecedented design of a Janus device; it involves fabrication of a sheet-like Janus device that has a dual layer consisting of mucoadhesion and omniphobicity at opposite sides.

### 1.3 Mucoadhesion

Mucoadhesion refers to adhesion to the mucosa or the mucus membrane, which is the moist tissue that lines body cavities and organs, such as the mouth, nose, lungs, and urinary and digestive tract.[15] To date, many studies have explored the optimum mucoadhesion considering the anatomical differences of the mucus membrane at different body regions.[15] A material's mucoadhesion may be affected by various factors, including molecular weight, hydrophilicity (through different functional groups like hydroxyl and carboxyl), pH, flexibility, cross-linking density, and charge and concentration of the active polymer.[16,17,18] Mucoadhesion can be measured and quantified by various evaluating methods, including tensile test, peel test, and shear experiments.[15] Additionally, *in vivo* evaluation with fluorescent imaging, radioactive imaging, magnetic resonance imaging, and transit time measurements can provide valuable information with respect to the transit times of mucoadhesives.[19,20,21]

In terms of drug delivery systems, mucoadhesives have been widely incorporated in drug formulations. Mucoadhesives for oral drug delivery can help lengthen gastric residence time of the drug delivery system and also control the rate of drug release in a specific targeted region.[16] Hence, mucoadhesives have the potential to enable prolonged drug bioavailability, which could help reduce the frequency of drug administration.[22] Additionally, they allow for a closer contact with the targeted tissue to attain rapid absorption and enhanced penetration of the delivered drug. In one study, Ahmed *et al.* used gastric retention formulations (GRFs), made of naturally occurring carbohydrate polymers and loaded with the model drug riboflavin, to study various properties and effects of mucoadhesives.[23] They carried out *in vitro* studies to examine swelling and dissolution characteristics and *in vivo* studies in fasted dogs as well as in healthy humans to assess gastric retention and drug release. The researchers found that when the GRFs were dried and immersed in gastric fluid, they swelled rapidly and released their drug content in a zero-order fashion for a period of 24 hours. Through *in vivo* studies using fasted dogs, they observed that the rectangular-shaped GRFs stayed in the stomach for more than 9 hours, while the other shapes including cubes, short and long cylinders were retained less than 2 hours. Ahmed *et al*. concluded that these GRFs demonstrated extended gastric residence time and increased bioavailability of drug compared to the immediate release formulations.

In another study, Salman *et al*. fabricated polymeric nanoparticle carriers with mucoadhesive properties to assess their adjuvant potential for oral vaccination.[24] These nanoparticles were coated with thiamine to target specific sites within the GI tract, focusing on Peyer's patches and enterocytes. The researchers studied the affinity of nanoparticles to the mucous membrane using orally inoculated rats. They concluded that the use of thiamine-

coated nanoparticles demonstrated promise as a delivery strategy for oral vaccination and immunotherapy purposes.

Mucoadhesive drug delivery systems have been developed in varying formulations, including powders, films, sprays, solid inserts, and gels.[25] Particularly for oral delivery, different dosage forms include patches, pastes, ointments, adhesive gels, mouth washes, films, and most commonly, tablets.[15] To achieve mucoadhesion in these systems, many natural and synthetic polymers have been employed, including: poly(ethylene glycol) (PEG), poly(vinyl alcohol) (PVA), poly(vinyl pyrrolidone) (PVP), poly(hydroxyethyl methacrylate) (PHEMA), and chitosan.[15]

Specifically for our drug delivery system, two methods will be used to achieve mucoadhesion. The first approach involves applying mussel-inspired surface chemistry with the use of a small-molecule ligand, dopamine; Figure 1-2 shows the chemical structure of dopamine.[26] The idea behind this chemistry was inspired by the composition of adhesive proteins in mussels that allows them to stick to virtually all types of inorganic and organic surfaces, wet or dry.[26] These proteins are known to be rich in 3,4-dihydroxy-L-phenylalanine (DOPA) and lysine amino acids. To mimic the adhesion provided by mussel proteins, dopamine has been used as a molecular building block for polymer coatings, as dopamine contains both amine ($-NH_2$) and catechol (-OH) functional groups. This biomimetic method is appealing for the fact that it does not require complicated chemical procedures. Through a simple dip-coating process in an aqueous solution of dopamine, it forms a thin surface-adherent polydopamine film on the substrate by self-polymerization. Studies have demonstrated the versatility of this method, as it has been used to form

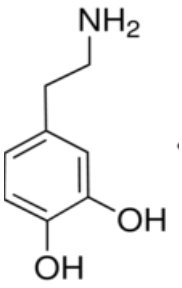


**Figure 1-2.** Chemical structure of dopamine.

multifunctional polymer coatings onto a wide spectrum of inorganic and organic materials, including noble metals, oxides, polymers, semiconductors, and ceramics. Also, this method has been used in therapeutic biomedical applications, such as stem cell and tissue engineering.[27,28]

The second approach involves using a well-accepted mucoadhesive polymer called Carbopol. Carbopol is an anionic polymer of acrylic acid lightly cross-linked with polyalkenyl ethers or divinyl glycol; Figure 1-3 shows the chemical structure of Carbopol.[29] Carbopol comes in the form of a white powder that can be easily pill-pressed into tablets. This mucoadhesive polymer can undergo a phase change from liquid to semisolid rapidly, demonstrating strong mucoadhesion when wetted.

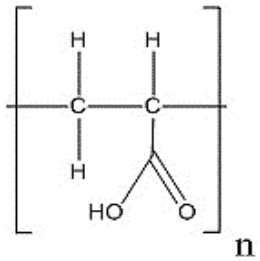

**Figure 1-3.** Chemical structure of Carbopol.

## 1.4 Omniphobicity

Unlike the wealth of applications utilizing mucoadhesion for the GI tract, the use of omniphobic (repellent to everything) surface coatings has been less explored. Specifically, the possible application of omniphobicity in drug delivery has not yet been reported. However, omniphobic materials have been studied for other applications. Some of the previously explored areas include non-wetting surfaces and biomedical fluid handling for applications in biomedical and optical devices.[30] Vogel *et al.* worked on fabricating a transparent coating that repelled a wide variety of liquids and prevented staining.[31] This coating also provided protection from mechanical damage and was capable of self-healing. In this example, omniphobicity was achieved by incorporating a colloidal monolayer that was backfilled with a silica precursor solution of tetraethylorthosilicate to build transparent, nanoporous surface structures. Through their study, a broad technological impact from solar

cell coatings to self-cleaning optical devices was envisioned. Moreover, other new potential applications of omniphobicity have been suggested and are being investigated, including for energy transition and environment-friendly manufacturing.[32]

Omniphobicity is much more difficult to obtain than hydrophobicity, for the surface has to repel other liquids, such as oil, as well as water. In order to understand the workings of omniphobicity, the behavior of hydrophobicity must first be understood. In the 1990s, the examination of a lotus leaf using scanning probe microscopy revealed that the ability of the lotus plant to repel water is a result of the tiny nano-structures on its leaf surface, called papillae.[33] This discovery has inspired a field of biomimetic research aimed at studying and fabricating "superhydrophobic" surfaces using the so-called "Lotus effect."[34] The Lotus effect refers to the superhydrophobic behavior demonstrated when the surface is wetted by water and a solid-air-liquid interface is formed, shown in Figure 1-4; this three-phase interface is explained by the Cassie-Baxter model of surface wetting.[35] The water droplet sits atop pockets of air trapped between the papillae and forms an almost perfect sphere. Thus, the contact area between the water and the surface has been drastically reduced, and the droplet can easily roll off the surface. However, superhydrophobic surfaces are unable to provide omniphobicity, as organic liquids, such as oil, are composed of nonpolar molecules that have much lower surface energy than the polar water molecules.[34] Consequently, it is not energetically favorable for oil droplets to remain as spheres on the solid surface.

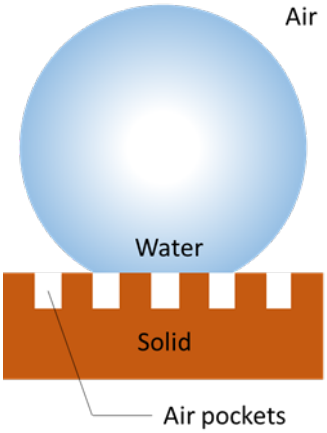


**Figure 1-4.** Solid-air-liquid interface, explained by the Cassie-Baxter model.

### 1.4.1 Omniphobicity for Our System: SLIPS

As described in the previous section, past studies have used the Lotus effect, in which a porous surface with arrays of nanoposts is created to give an air-liquid interface that would not be wetted by water.[34] In addition to hydrophobic surfaces, researchers have developed surfaces that are not wetted by a broad range of liquids and are therefore named "omniphobic."

To achieve omniphobicity in our Janus device, we adapted the Slippery Liquid-Infused Porous Surface (SLIPS) system, described by Wong *et al.*[30] Inspiration of the SLIPS came from the *Nepenthes* plant, a carnivorous pitcher plant that has micro-structures on its surface. These micro-structures can lock in a liquid layer to create a slick coating on which the prey will slip and fall into the plant. Similar to the plant, by applying a lubricating film of

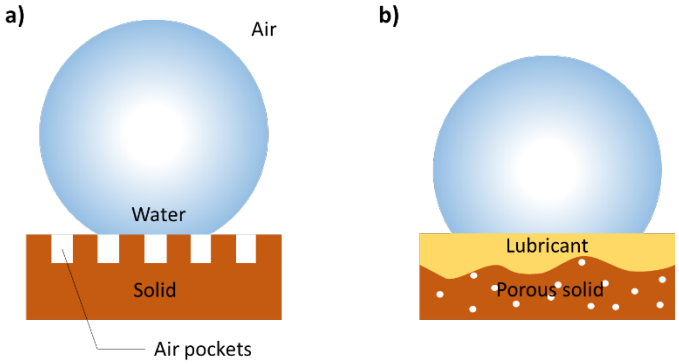


**Figure 1-5.**
**(a)** Hydrophobicity achieved through an air-liquid interface of Lotus effect versus **(b)** Omniphobicity achieved through a liquid-liquid interface with the addition of a lubricant.

perfluorinated liquid in addition to the nanoposts, the SLIPS system managed to achieve omniphobicity through creating a liquid-liquid interface, shown in Figure 1-5(b). The SLIPS system gave a low-cost way to create a self-healing surface with durability to sustain physical stress and pressure.

### 1.4.2 Characterization of Omniphobicity

Omniphobicity can be confirmed by contact angle goniometry, illustrated in Figure 1-6; this technique characterizes the strength of interaction of the liquid-solid interface. The instrument dispenses a small fixed volume droplet of the chosen liquid onto the surface of the substrate and then measures the angle made between the line tangent to the small liquid droplet and the surface. The contact angle measurement provides information on the relative hydrophilicity, hydrophobicity, and omniphobicity of the substrate surface. Figure 1-7 gives ranges of contact angle values and their corresponding surface characteristics when water is used to test the hydrophilicity or hydrophobicity of a surface.[36,37] A surface that is omniphobic will show a non-zero contact angle when wetted by organic liquids, such as oil and hexane, along with a high contact angle when wetted by water. Static and dynamic contact angles with various polar and non-polar liquids, including water, acid and bases, organic solvents, and oil, will be measured to characterize the substrate surface.

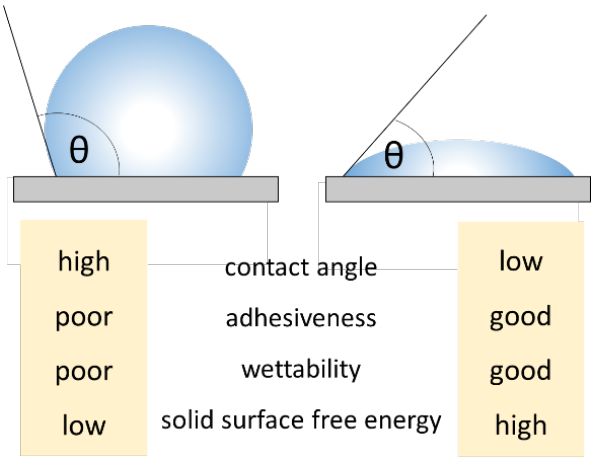


**Figure 1-6.** Schematic of contact angle goniometry measurement. Adapted from *Ramé-Hart Instrument Co.*

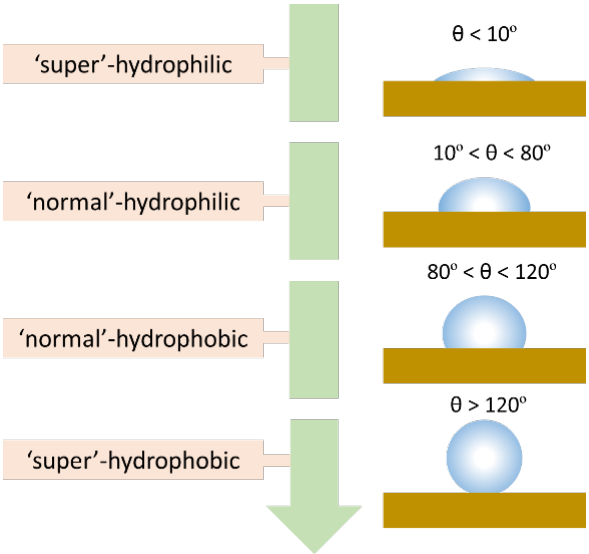


**Figure 1-7.** Contact angle values with their corresponding surface characteristics when water is used to test the hydrophilicity or hydrophobicity of a surface. The blue droplets represent water.

## 1.5 Gastrointestinal (GI) Tract – Esophagus System

The human GI tract can be subdivided into four major components: esophagus, stomach, small intestine, and large intestine. Our project specifically concentrates on providing drug delivery for the esophagus portion within the GI tract, highlighted in Figure 1-8. The esophagus has been overlooked as a site for drug delivery in comparison to the rest of the GI tract because of the great challenges associated with it.[38] The esophageal tube is approximately 25 centimeters long and 2 centimeters wide and has a pH level of 6 to 7.[39] As the first conduit for the GI tract, the esophagus transports rough, undigested food. This exposes the esophagus to heterogeneous materials passing through the narrow tube in a matter of a few seconds. The transit times range from 4 to 8 seconds for solids and 1 to 2 seconds for liquids in a healthy human body.[40] Moreover, the stratified squamous mucosal surface is not ideal for systemic drug absorption.[38] With these challenging conditions, a greater need arises for stronger and extended adhesion of the drug delivery device to the esophageal mucosa.

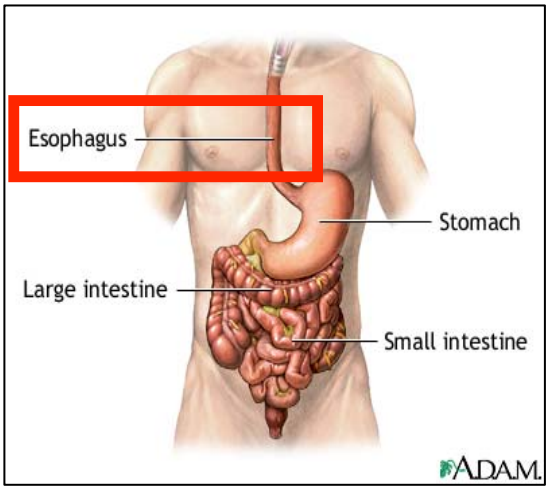


**Figure 1-8** . Human GI tract, highlighting the esophagus. Adapted from *A.D.A.M.*

A range of delivery approaches for targeting the esophagus have been previously explored. These include films, gels, adhesive liquids, chewing gums, orally retained lozenges, and also endoscopically delivered therapeutics.[41] In the case of treatment for gastroesophageal reflux system, the liquid formulations adhere to the esophageal mucosa and provide a protective coating against refluxed gastric content.[38] Success in achieving such a localized drug delivery has the capacity to fill a significant unmet need with the potential to

improve morbidity and mortality from esophageal diseases, including esophageal cancers, allergic conditions such as eosinophilic esophagitis, and even the more common reflux diseases that are all associated with medication non-compliance.[42] Furthermore, the development of devices compatible with esophageal delivery would be directly applicable to delivery in the rest of the GI tract, thereby providing a universal platform for GI-based drug delivery.

### 1.6 System Design

Although many previous studies have already been conducted in each individual field of Janus particles, mucoadhesion, omniphobicity, and esophageal drug delivery, no work that integrates all these components has yet been reported. The novelty of this project is found in the unprecedented idea of engineering a drug-delivery Janus device with both omniphobic and adhesive sides for biomedical applications in the esophageal system.

To achieve the goal of developing a drug-delivery vehicle that has the unique capacity for extended GI retention, our project will advance in three phases. First, for material synthesis, the system illustrated in Figure 1-9 will be constructed. A flat dual layer will be fabricated, in which one side is mucoadhesive, enabling adhesion to the GI mucosa, and the other side is omniphobic, repelling foodstuffs and bodily secretions traveling rapidly down the esophagus. A polymer loaded with the drug will be located between the two layers of the device; this

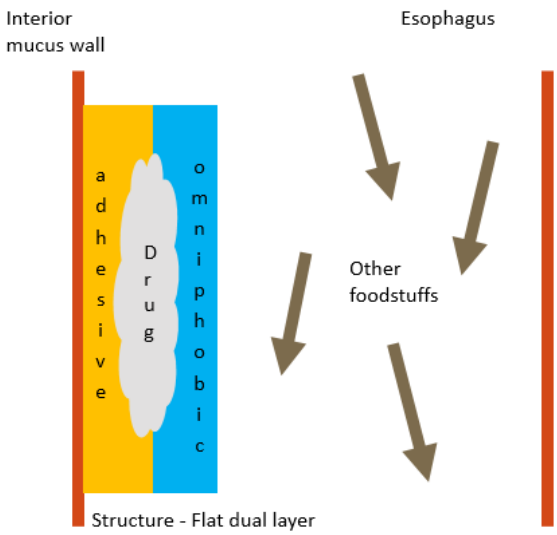


**Figure 1-9.** Schematic design of the Janus drug-delivery system.

polymer will allow controllable release of the desired drug. The next phase involves conducting *in vitro* dislodgement tests with a simulated gastric model using pig esophageal and intestinal tissues, as the GI tract of pigs is most equivalent to that of humans.[43] In the final phase, the efficacy of the fabricated Janus device will be assessed using porcine and rodent models *in vivo*, in which the stability and drug release of the device in the native GI environment will be evaluated.

### 1.7 Criteria for the Optimal GI Compatible Polymer

As described in the previous section, the purpose behind the schematic design of the proposed Janus system is to provide a facile approach to develop a novel drug-delivery device that would avoid easy detachment by and aggregation with foodstuffs in the GI tract. With that purpose in mind, it is crucial to choose a polymer that is optimal for the proposed system. This polymer would be used to construct the omniphobic side and be loaded with the drug for a controllable release. The criteria for the optimal polymer are that it must be GI compatible and robust, which means that it must be able to endure the acidic conditions of the GI tract, as well as be biocompatible and biodegradable. The polymer also must be able to be loaded with drug, which means that the use of heat should not be required for its polymer casting process. Furthermore, the optimal polymer should have hydroxyl (-OH) or/and carboxyl (-COOH) functional groups. Finally, the casting process should be simple and inexpensive.

All of the components listed in the criteria are self-explanatory, except for the need of hydroxyl and carboxyl functional groups. To expand on the desirability of hydroxyl and carboxyl functional groups for the polymer, we must think about the fluorination step of the

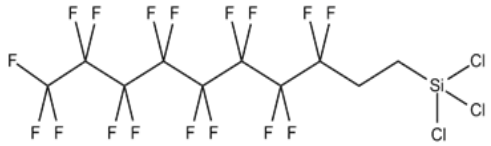


**Figure 1-10:** Chemical structure of heptadecafluoro-1,1,2,2-tetrahydrodecyl trichlorosilane.

fabrication process. The hydroxyl and carboxyl functional groups allow the polymer to be more easily fluorinated. The fluorination step is required to create an omniphobic surface and involves using the chemical heptadecafluoro-1,1,2,2-tetrahydrodecyl trichlorosilane. As shown in Figure 1-10, this molecule has a silane group at one of its ends. Consequently, through silane chemistry,

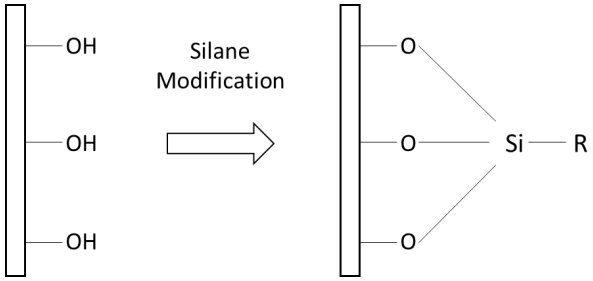


**Figure 1-11:** Schematic diagram depicting how silane modification works with hydroxyl groups on the substrate surface.

the fluorinated substrate can undergo a condensation reaction, drawn out in Figure 1-11. Thus, hydroxyl or carboxyl groups are desirable for the substrate to enable silane modification.[44] In the process of drafting the protocol to fabricate our proposed Janus device, different types of polymers will be considered and compared for different characteristics in order to choose the polymer that is optimal for our system.

# 2. MATERIALS AND METHODS

## 2.1 Materials

Nanopure water was used for all aqueous sample preparations and experiments (Millipore Milli-Q Reference Ultrapure Water Purification System, 18.2 MΩ·cm). Acetone (AR, ACS grade) was purchased from Macron Fine Chemicals (Center Valley, PA). Dichloromethane (HPLC grade, ≥ 99.8%) was obtained from EMD Chemicals (Gibstown, NJ).

For creating polydimethylsiloxane (PDMS) molds, Sylgard 184 Silicone Elastomer Kit was used with the base and the curing agent purchased from Dow Corning (Midland, MI). Fresh lotus leaves were acquired from a local company called Wonderful Water Lilies (Sarasota, FL), privately owned by Marilyn Eigsti.

Poly(lactide-co-glycolide) (PLGA) (85:15, 2.22 dL/g, ester end) was purchased from Hangzhou Hysen Pharma Co., Ltd. (Hangzhou, China). Cellulose acetate (MW~30,000) was purchased from Sigma-Aldrich (St. Louis, MO). For functionalizing surfaces for omniphobicity, heptadecafluoro-1,1,2,2-tetrahydrodecyl trichlorosilane was purchased from Gelest, Inc. (Morrisville, PA), and 100% Fluorinert FC-70 Fluid was purchased from Hampton Research (Aliso Viejo, CA). For adhesive surfaces, Carbopol 934 was purchased from Lubrizol (Wickliffe, OH) and dopamine hydrochloride was purchased from Sigma-Aldrich. Tris buffer (10 mM Tris, pH 8.5) was prepared by mixing Trizma Base, purchased from Sigma-Aldrich, with nanopure water. The reducing agent, sodium cyanoborohydride (reagent grade, 95%), was obtained from Sigma-Aldrich. All chemicals were used as received unless otherwise specified.

For *in vitro* studies, pig tissues, including small intestine and esophagus, were procured from a local slaughterhouse in Massachusetts. All tissues were collected within 2 hours of the animal being sacrificed and kept at 4 ºC for as long as 7 days. All animal tissue work was approved by MIT's Institutional Animal Care and Use Committee (IACUC), the Committee on Animal Care (CAC).

## 2.2 Fabrication of Omniphobic Surface

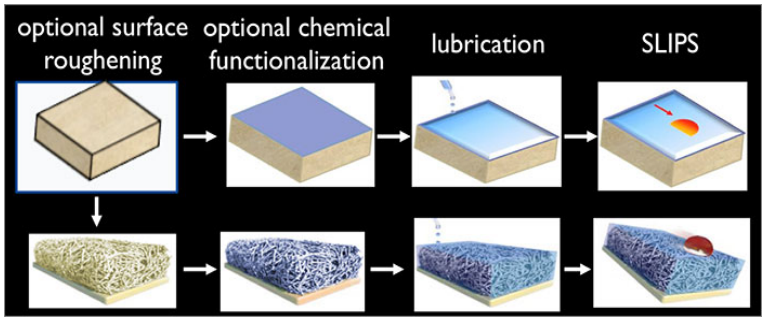


**Figure 2-1.** Steps involved in creating the SLIPS system. Adapted from Wong *et al.*[30]

As described in section *1.4.1* and shown in Figure 2-1, the omniphobic surface was fabricated adapting a modified version of the SLIPS system by Wong *et al.*[30] For surface roughening, a polymer surface with an array of nanoposts was created using a cured PDMS mold. Then, this epoxy-replicated nanoarray, which is now superhydrophobic, was chemically functionalized through fluorination and lubrication, making the surface omniphobic.

### 2.2.1 Surface Roughening

As illustrated in Figure 2-2, the technique of soft lithography was used for surface roughening. In order to create a polymer surface with nanoposts, a negative replica of a PDMS mold was needed. The natural lotus leaf was cut into a small piece, rinsed with nanopure water, and dried with nitrogen gas. Then, the leaf was glued down to a plate with the upper leaf side facing out for an imprinting procedure. PDMS solution was made with 10:1 ratio of Sylgard 184 Silicone Elastomer base and curing agent.

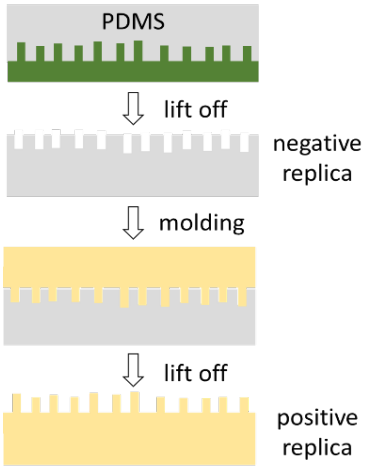


**Figure 2-2:** Schematic illustration of the procedure for nanocasting PDMS negative replica and then nanocasting polymer positive replica from the cured PDMS mold.

Then, the PDMS solution was placed in a vacuum desiccator for approximately an hour to eliminate air bubbles within the solution. Afterward, the solution was poured onto the plate with the leaf taped down on the bottom. The mold was placed in a vacuum oven at 40 ºC overnight. After being taken out of the oven, the mold was placed at room temperature for an hour to cool down before it was peeled off from the leaf. This cured PDMS mold represented the lotus leaf imprint.

Once the lotus leaf imprint was completed, either PLGA or cellulose acetate films were made by solvent-casting. For PLGA films, PLGA was dissolved in dichloromethane at a concentration of 50 mg/mL. The solution was stirred for an hour at room temperature until no solids could be seen. The solution was poured onto the PDMS mold, and the mold was placed in a 60 ºC oven until all dichloromethane was evaporated. For cellulose acetate films, the cellulose acetate solution of 40 mg/mL was prepared in acetone. The solution was stirred for an hour at room temperature until no solids could be seen. The cellulose acetate solution was poured onto the PDMS mold and air-dried for an hour at room temperature until all acetone was evaporated. Then, the polymerized film, either PLGA or cellulose acetate, was peeled off from the mold, creating a positive replica with the array of nanoposts.

### 2.2.2 Chemical Functionalization

The polymer positive replica with nanoposts was fluorinated by placing it in a vacuum desiccator overnight with 0.2 mL of heptadecafluoro-1,1,2,2-tetrahydrodecyl trichlorosilane in a glass vial. Then, the Fluorinert FC-70 Fluid was pipetted over the fluorinated surface to create a lubricating film locked within the nanoposts. Thus, the omniphobic surface was fabricated.

## 2.3 Fabrication of Mucoadhesive Surface

As described in section *1.3*, the procedure from the mussel-inspired surface chemistry was used to form an adherent polydopamine coating that binds to the substrate. First, PLGA was dissolved in dichloromethane at a concentration of 50 mg/mL. The solution was stirred for an hour at room temperature until no solids could be seen. The solution was poured onto a flat PDMS mold to be solvent casted. The mold was placed in a 60 ºC oven until there was a complete evaporation of the solvent and PLGA was fully polymerized into a thin film. Then, the PLGA substrate was immersed in the solution of 2 mg/mL dopamine hydrochloride with 10 mM Tris buffer at pH 8.5. The solution was left stirring slowly overnight at room temperature. Subsequently, the coated polymer was gently rinsed with nanopure water to remove any unattached dopamine molecules.

### 2.3.1 Prevention of Oxidation

To avoid oxidation of the dopamine, which can be noted by the color change of the sample to dark brown, an excess amount of sodium cyanoborohydride as a reducing agent was mixed into the dopamine solution. Throughout the experiments, all dopamine solutions were deoxygenated by continuously bathing with nitrogen gas. When not in active use, all dopamine solutions were stored inside a vacuum desiccator, minimizing oxygen gas exposure.

### 2.3.2 Alternative Approach for Mucoadhesion

As an alternative method to the use of dopamine, a commercial mucoadhesive polymer, Carbopol, was used to attain mucoadhesion. Here, approximately 500 mg of Carbopol was pill-pressed into a tablet, at 20 MPa, using the YLJ-24T Desk-Top Powder Presser purchased from MTI Corporation.

## 2.4 Fabrication of Janus Devices

The protocol to create a Janus device that is adhesive on one side and omniphobic on the other side was designed. Since Carbopol and cellulose acetate are both in powdered form, with the Carbopol powder on the bottom layer and cellulose acetate powder on the top layer, they were pill-pressed into a dual-layer thin tablet. A droplet of acetone was pipetted onto the surface of the cellulose acetate layer. Then, the tablet was quickly pressed into the PDMS lotus leaf mold with the wetted cellulose acetate layer facing down onto the mold. The tablet was pressed down for approximately 15 minutes until the acetone evaporated away. The tablet was detached from the PDMS mold and fluorinated and lubricated following the protocol stated in section *2.2.2.*

## 2.5 Surface Characterization

The morphology of the fabricated surfaces was observed by the means of the JEOL 5600LV Scanning Electron Microscope (SEM) located in the facilities at MIT Whitehead Institute, Cambridge, MA. Before visualization under SEM, all samples were sputter-coated with carbon using the Hummer 6.2 Sputter Coating System. Samples were cut to be under ~0.5 $cm^2$ in area and fixed to the aluminum stubs by double-sided adhesive carbon conductive tape.

Fabricated surfaces were characterized for the degree of adhesiveness, hydrophobicity, and omniphobicity by taking the static contact angle measurements by the means of the Krüss Drop Shape Analyzer DSA100 with the software Drop Shape Analyzer (Matthews, NC). Contact angles of various liquid (water, organic solvents, and oil) droplets over the sample surface, fixed to lay flat on a horizontal plane, were measured at room temperature. A

fixed volume of ~250 µL droplet of the chosen liquid was dispensed onto the substrate, and then the contact angle made between the line tangent to the liquid droplet and the substrate surface was measured. The macroscopic droplet profile was photographed by a camera installed within the instrument. A sample image is shown in Figure 2-3. For each surface, five contact angle measurements were taken. The average and the standard deviation values for each surface were calculated and reported.

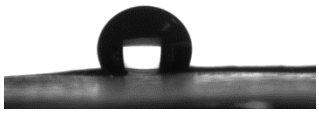

**Figure 2-3:** An example of real-time macroscopic droplet profile image for contact angle measurement.

## 2.6 *In Vitro* Studies Apparatus

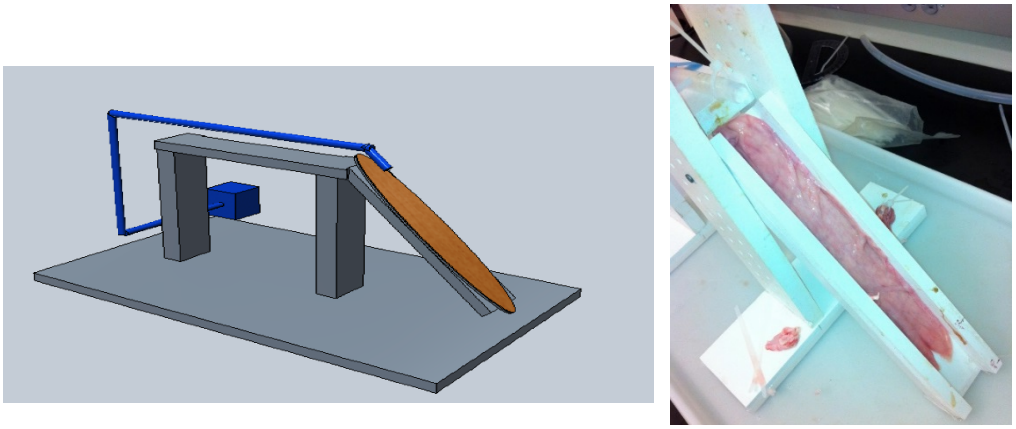

**Figure 2-4.** Apparatus for *in vitro* studies using porcine tissues.

Macroscopic *in vitro* evaluation was carried out by using a self-built apparatus shown in Figure 2-4. Small intestinal tissue from a porcine model was cut into the length of 30 cm and sliced opened to line the angled slide of the apparatus. A Janus device (omniphobic and adhesive) and a non-Janus device (adhesive on both side) were placed at the same distance of 22 cm from the bottom of the slide. In order to simulate the aggregation with the foodstuffs expected when the device is attached to the GI mucosal wall, a solid object of same mass was

purportedly placed on top of each sample. The weight also served to speed up dislodgement and to demonstrate adhesion or omniphobicity on the side facing up. A Masterflex L/S Variable-Speed Drive peristaltic pump, purchased from Cole-Parmer, was set up with some tygon tubing. The pump operated at the constant speed of 85 rpm and flowed water over the tissue. The times of dislodgment were documented and compared for the two different devices. Video was recorded by a hand-held digital camera and sequential photographs from the video recordings were collected.

# 3. RESULTS AND DISCUSSION

## 3.1 Creating Epoxy-replicated Nanoarray

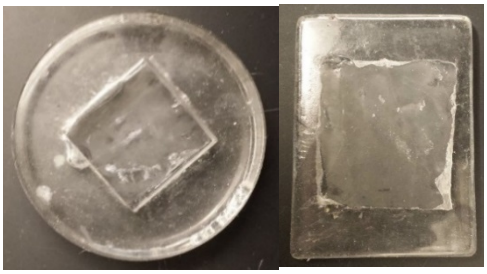

**Figure 3-1.** PDMS molds with nanowells made from a lotus leaf template.

As described in section *1.4.1*, the SLIPS system requires an epoxy-replicated array of nanoposts before fluorinating the surface and applying the lubricating film. The original procedure described by Wong *et al*. involved carrying out lithography using a silicon wafer, but we aimed to develop a more low-cost and facile method. We avoided purchasing a silicon wafer and instead used soft lithography with a fresh lotus leaf template to create a negative replica of PDMS mold with nanowells, shown in Figure 3-1. Multiple attempts with different order of steps and varying degrees of temperature, curing time, and PDMS solution ratio of base and curing agent were tried until a feasible protocol (outlined in section *2.2.1*) successfully produced a stable PDMS mold that could morphologically replicate the nano-structures on the lotus leaf.

3.1.1 Verification of Negative and Positive Replicas

Through soft lithography, negative and positive replicas were made using a lotus leaf template. Since the nano-structures on the lotus leaf were too small to be directly visualized, SEM served as a useful tool to monitor and verify the morphological replication of the structures. Also, contact angle measurements, where the mean values and standard deviations were reported along with the representative droplet profiles, were used to examine the changed surface characteristics. The surfaces were characterized by comparing their measured contact angles with those previously reported in literature, organized into ranges in Figure 1-7.[36,37]

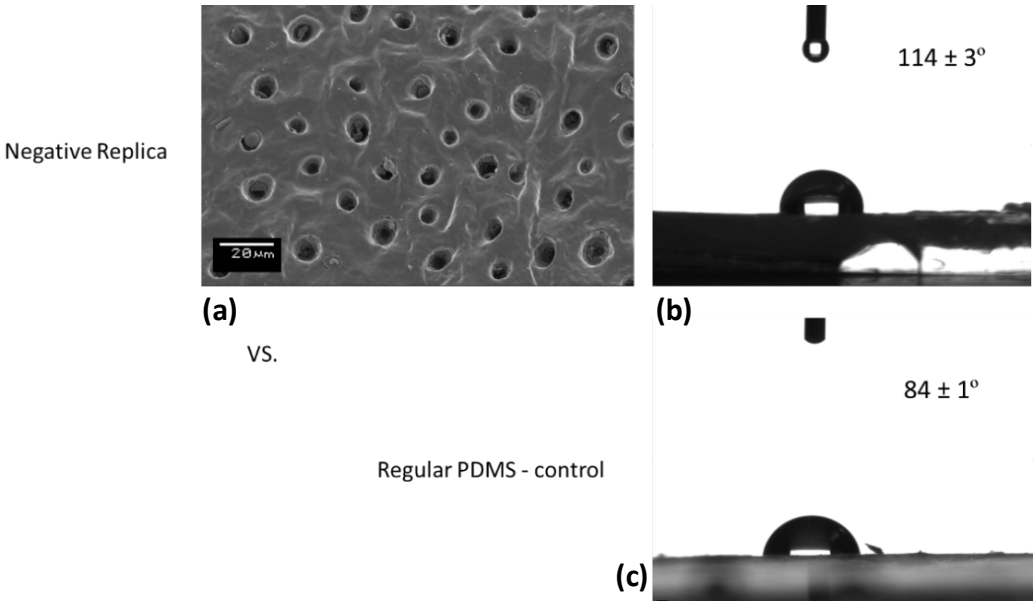


**Figure 3-2.** (a) SEM image of the nanowells on the negative PDMS replica. (b) Contact angle measurement of the negative PDMS replica compared to (c) contact angle measurement of a control PDMS. The mean values and standard deviations of the contact angles are reported (n = 5).

The negative replica, which is the PDMS mold made from the lotus leaf imprinting process, was expected to demonstrate nanowells. The SEM image in Figure 3-2(a) confirmed that the nanowells were successfully created on the PDMS mold surface. Since the surface was roughened by the nanowells and thus made more hydrophobic, compared to a regular PDMS polymer, we expected to see an increase in the contact angle measurement. First, the

innate hydrophobic nature of the PDMS material was verified; the unmodified control PDMS surface showed a contact angle of 84 ± 1º, seen in Figure 3-2(c). For the PDMS mold with the nanowells, we observed the expected increase in the contact angle to 114 ± 3º, seen in Figure 3-2(b); the contact angle increased by 30º. The literature reported contact angle values of ~100º for the control PDMS and ~124º for the PDMS surface with nanowells, which gave an increase of 24º.[45] The deviation of our contact angles from the literature values was hypothesized to be attributed to the different type of silicone elastomer and different molding method used in the literature study.[45] However, with a similar increase in the contact angles between the control and the modified PDMS, we could conclude that our experimental values for the negative replica showed a comparable behavior to the literature values.

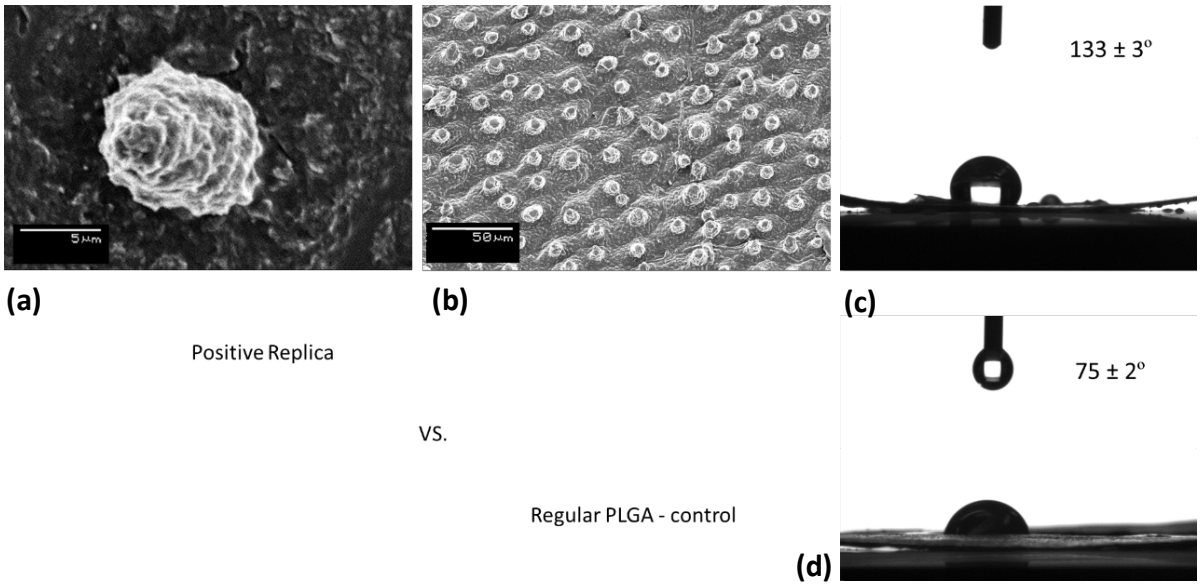


**Figure 3-3.** SEM images at (a) high magnification of a single nanopost on the positive PLGA film replica and (b) low magnification of the nanoposts on the positive PLGA film replica. (c) Contact angle measurement of the positive PLGA replica compared to (d) contact angle measurement of a control PLGA. The mean values and standard deviations of the contact angles are reported (n = 5).

The positive PLGA film replica prepared from the negative replica of the lotus leaf PDMS mold was expected to demonstrate nanoposts. The SEM images in Figure 3-3(a,b) confirmed that the nanoposts were successfully created on the surface of the positive replica.

Since the surface is roughened by the nanoposts and thus made superhydrophobic (>120º from Figure 1-7), compared to a regular PLGA polymer, we expected to see an increase in the contact angle measurement.[45] The innate hydrophobic nature of PLGA material was verified, as the unmodified control PLGA surface showed a contact angle of 75 ± 2º, seen in Figure 3-3(d). The control PLGA surface had an intrinsic contact angle close to the values of 75º–84º found in the literature.[46,27] For the PLGA polymer with the nanoposts, we observed a contact angle of 133 ± 3º, seen in Figure 3-3(c); the contact angle increased by 58º. As discussed in section *1.4,* the effect of superhydrophobicity introduced by the Lotus effect or the addition of nano-structures was observed.[45] The contact angle of the positive PLGA replica (133 ± 3º) was comparable to the contact angle of the natural lotus leaf at 147 ± 3º,

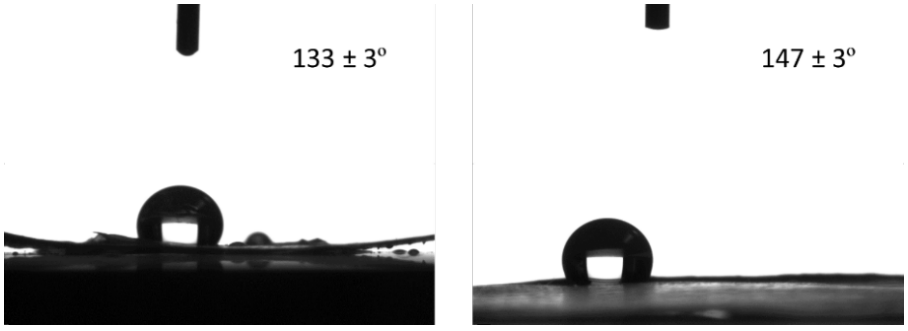


**Figure 3-4.** Contact angles of the positive PLGA replica (left) and the natural lotus leaf (right). The mean values and standard deviations of the contact angles are reported (n = 5).

shown in Figure 3-4. A difference of 14º was hypothesized to be attributed to either the material difference between the leaf and PLGA or the loss in the nanoposts' height during the casting process; this was investigated further in the following section *3.1.2*. Ultimately, all these findings indicated that the soft lithography process successfully replicated the morphology of a natural lotus leaf in creating a surface with an epoxy-replicated nanoarray.

3.1.2 Magnification of the Nano-structures

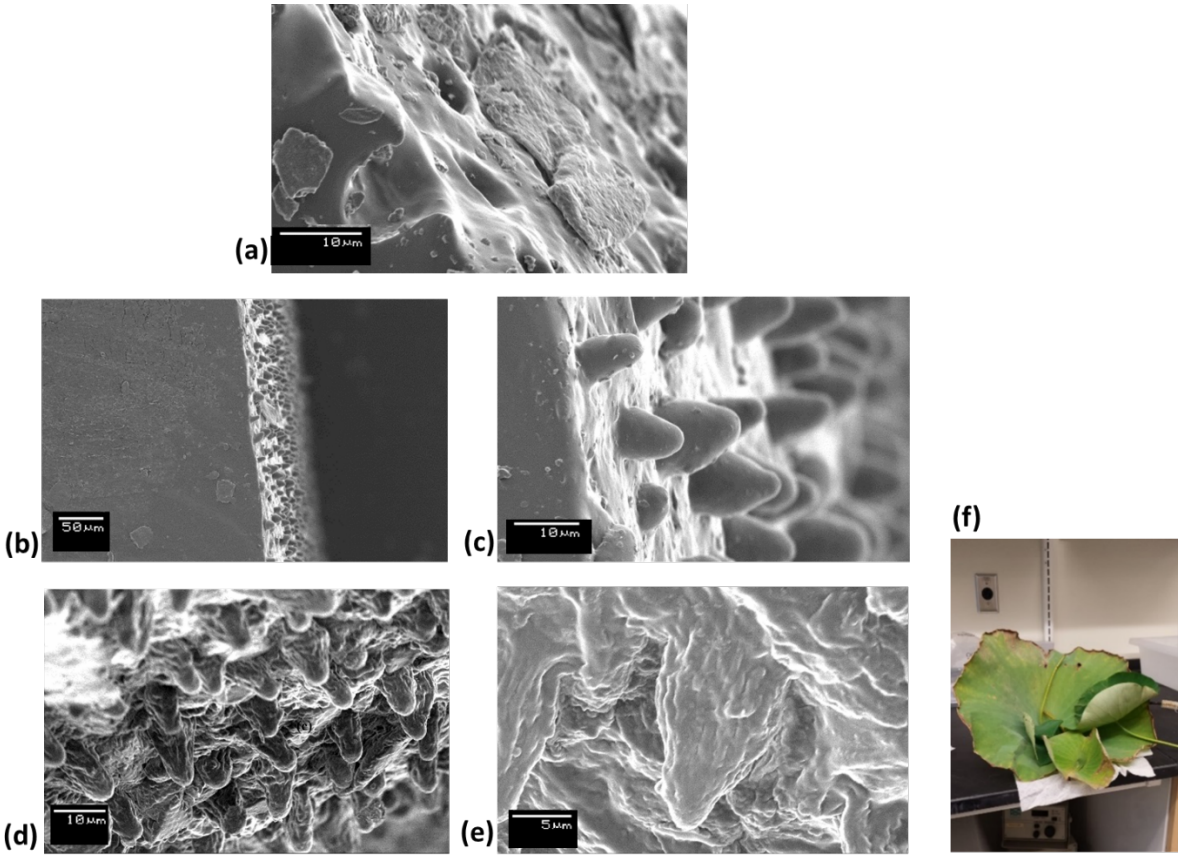


**Figure 3-5.** SEM images at: (a) high magnification of the nanowells on the negative replica surface, (b) low magnification of the nanoposts of the positive replica surface, (c) high magnification of the nanoposts on the positive replica surface, (d) low magnification of the nanoposts on the natural lotus leaf surface, and (e) high magnification of the nanoposts on the natural lotus leaf surface. (f) A photograph of the natural lotus leaves.

The replication quality of the nano-structures on the lotus leaf was assessed by the SEM images, displayed in Figure 3-5. The SEM images were analyzed visually using the appropriate scales on the images and measuring the approximate heights of the nanostructures for each image. Orthogonally tilted SEM images demonstrated that there was no loss in the height of the nanoposts created by soft lithography. The approximate height of 10 μm was maintained throughout the molding process, as observed: the initial height of 10 μm on the surface of the natural lotus leaf in Figure 3-5(e), the depth of 10 μm of the nanowells on the negative replica in Figure 3-5(a), and the height of 10 μm of the replicated

nanoposts on the positive replica in Figure 3-5(c). Magnification SEM images confirmed that the nano-structures were transferred without damages or irregularities throughout the molding process. Therefore, it was concluded that the replication of these nano-structure was at a high quality.

### 3.2 Omniphobic Side

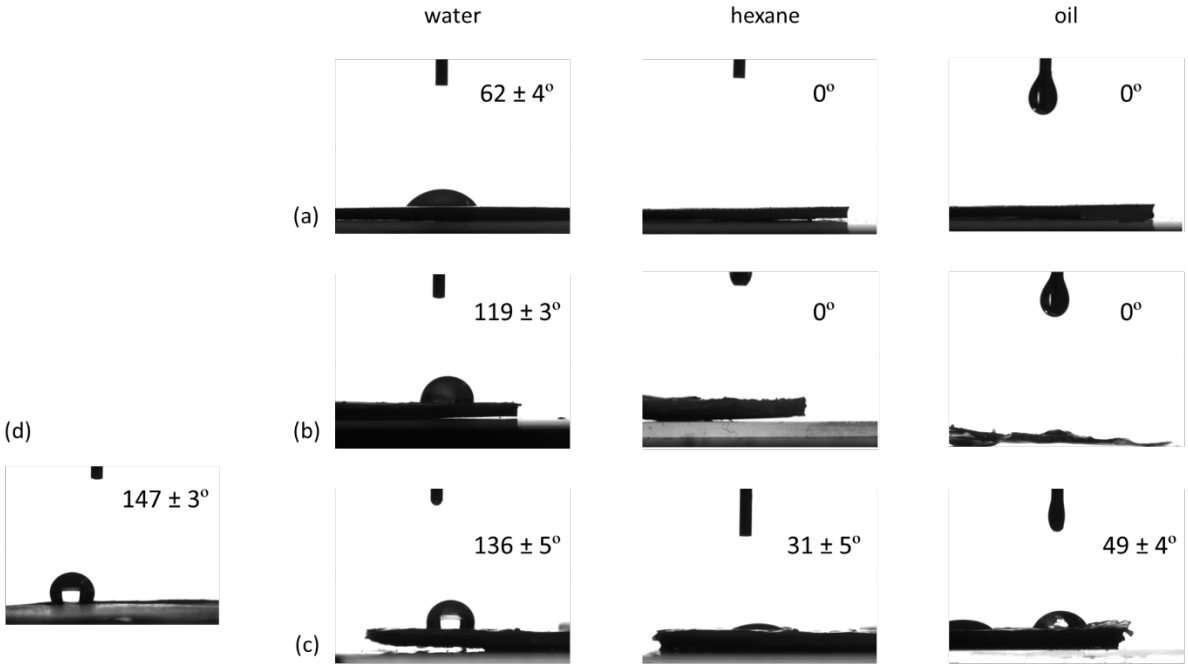


**Figure 3-6.** Contact angle measurements of: (a) cellulose acetate without nanoposts, (b) hydrophobic surface - cellulose acetate with nanoposts, (c) omniphobic surface - cellulose acetate with nanoposts *via* SLIPS system, and (d) natural lotus leaf, using different liquids (water, hexane, and oil). The mean values and standard deviations of the contact angles are reported (n = 5).

As described in section *1.4.2*, contact angle goniometry was used to examine the changed surface characteristics and to confirm omniphobicity. Omniphobic surface would show a high contact angle with water and non-zero contact angles with organic liquids. In Figure 3-6, the contact angle measurements, using different liquids (water, hexane, and oil), of the cellulose acetate surfaces modified in various ways were compared to the contact angle measurement of the natural lotus leaf. The mean values and standard deviations were

reported along with the representative droplet profiles. Row (a) represents a regular flat cellulose acetate surface. While the contact angle with water was 62 ± 4º, the contact angles with hexane and oil were both 0º. Row (b) represents a hydrophobic surface, which is the cellulose acetate surface with nanoposts. Even though the water droplet displayed an increased contact angle of 119 ± 3º due to surface roughening, the contact angles of both hexane and oil still remained at 0º. Row (c) represents an omniphobic surface, which is the cellulose acetate surface with nanoposts that has also been fluorinated and lubricated. Not only did the contact angle of the water droplet increase to 136 ± 5º, but also the contact angles of both hexane and oil were no longer 0º. The hexane droplet showed a contact angle of 31 ± 5º and the oil droplet showed a contact angle of 49 ± 4º. The retention of both water and organic liquids as visible droplets on the surface supports the fact that omniphobicity was achieved by surface morphological and chemical modifications.[30]

### 3.3 Mucoadhesive Side

To obtain mucoadhesion, mussel-inspired surface chemistry (described in section *2.3*) was initially investigated, where the substrate was dip-coated in a dopamine solution to form a surface-adherent coating. The contact angle analysis of the dopamine-coated polymer indicated a possible sign of mucoadhesion. As seen in Figure 3-7, a regular PLGA film showed a contact angle of 75 ± 2º, compared to the literature value of 75º–84º.[46,27] The dopamine-coated PLGA showed a significantly decreased contact angle of 33 ± 4º, which was comparable to

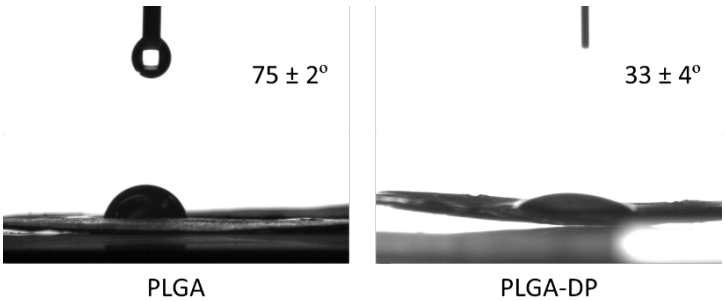


**Figure 3-7.** Contact angle measurements of PLGA (left) and dopamine-coated PLGA (right). The mean values and standard deviations of the contact angles are reported (n = 5).

the literature value of 26º.[27] The decrease in the contact angle signified that the surface was no longer hydrophobic.

However, by visual observation and simple qualitative testing on the porcine small intestinal and esophageal tissues, the dopamine-coated polymer showed no strong mucoadhesion. Notably, the dopamine solutions and the functionalized polymers turned dark brown continuously during many trials, as shown in Figure 3-8. Based on some literature studies, we speculated that the most plausible reason for the lack of strong mucoadhesion was oxidation of the catechol groups (-OH) on the dopamine molecules.[47,48] As explained in section *1.3,* amine and catechol functional groups are key components for adhesion in mussel-inspired surface chemistry. The literature also indicated that the color change to dark brown is an apparent sign of oxidation.[47] A notable observation during the literature studies was that no literature could be found, in which this mussel-inspired surface chemistry was tested on porcine tissues.

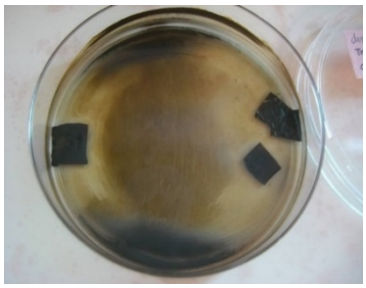

**Figure 3-8.** Oxidized dopamine solution and dip-coated polymer substrate, indicated by the dark brown color.

Thus, steps were taken to prevent oxidation by using nitrogen gas to deoxygenate the dopamine solution and also mixing in an excess amount of a reducing agent, sodium cyanoborohydride, into the solution during the dip-coating process.[49,50] Furthermore, precautionary measures, such as placing all dopamine solutions when not in active use in a vacuum desiccator, were taken. However, even though these measures prevented the color change, the functionalized polymer still did not demonstrate strong mucoadhesion when tested qualitatively. For continuance of this method in the future, other measures to minimize oxidation could be tested, such as chemically modifying the dopamine molecules into

dopamine methacrylamide (DMA) or halogenating the dopamine molecules with chlorine. These were suggested in literature as potential steps to prevent oxidation of the dopamine molecules.[48,51] Alternatively, Carbopol, a well-accepted mucoadhesive polymer that showed strong adhesion when wetted, was instead used for our experiments.

### 3.4 Choosing the Optimal GI Compatible Polymer

As described in section *1.7*, the polymer that would be used to construct the omniphobic side and loaded with drug must be chosen carefully to carry out the purpose of our system. The criteria for the optimal polymer listed in section *1.7* were that it must be GI compatible, biocompatible, biodegradable, and durable. The polymer also must be able to be loaded with drug, which meant that heating should be avoided. Furthermore, the ideal polymer should have hydroxyl (-OH) or/and carboxyl (-COOH) functional groups. Finally, the casting process should be simple and inexpensive.

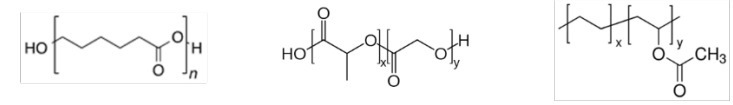

**Poly(caprolactone) PCL**
- inexpensive
- biocompatible
- biodegradable
- hydrophobic

- too fragile
- very slow drug release

**Poly(lactic-co-glycolic) acid PLGA**
- biocompatible
- biodegradable
- hydrophobic

- expensive
- hard to work with

**Poly(ethylene-co-vinyl acetate) PEVA**
- inexpensive
- biocompatible
- hydrophobic

- requires high heating
- not degradable

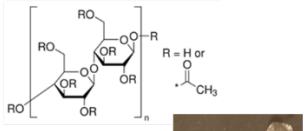

**Cellulose acetate**
- inexpensive
- biocompatible
- biodegradable
- hydrophobic
- not too fragile
- soluble in acetone (fast solvent evaporation)
- have -OH
- powder form

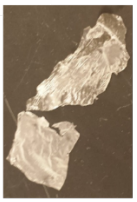

**Figure 3-9:** Table of candidates for the optimal GI compatible polymer with their characteristics

For the consideration of the optimal polymer, four types of polymers that are common in drug delivery were considered and compared in terms of different aspects, listed out in Figure 3-9. Amongst the four, cellulose acetate satisfied all of the key criteria. Specifically,

the material is inexpensive, biocompatible, biodegradable, intrinsically hydrophobic, not too fragile, and has hydroxyl functional groups. Additionally, it is soluble in acetone, a quickly evaporating solvent, and it is in a powdered form like Carbopol, which is convenient for the fabrication process using a pill presser. This justified our choice of cellulose acetate as the optimal GI compatible polymer to be used in the fabrication process of the Janus device. To test and demonstrate the compatibility of cellulose acetate with our proposed system, cellulose acetate was casted into a thin film and put through the imprinting process, described in section *2.2.1*. As seen in Figure 3-10, the SEM image of the modified cellulose acetate surface showed a sign of surface roughening with the creation of the nano-structures, similar to those on the lotus leaf. Thus, the SEM analysis verified that nanoposts can be successfully replicated on cellulose acetate.

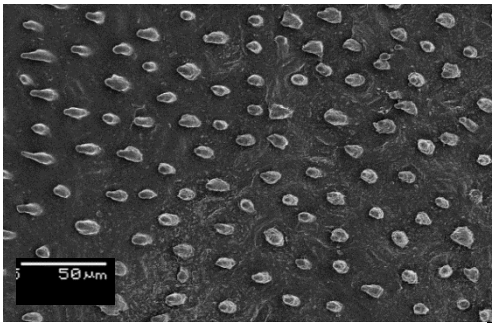


**Figure 3-10.** SEM image of the nanoposts on the cellulose acetate polymer surface.

### 3.5 Design and Fabrication of Janus Device

Through multiple variations in polymers, solvents, casting times, and orders of steps, a feasible protocol was finally designed and verified to see that it creates a sturdy model of the Janus device, as shown in Figure 3-11. This protocol, outlined in section *2.4*, should allow drug delivery with tunable loading capacity, including adjustable amount of drug loaded, controllable release of the desired drug, and protection of the drug from acidic conditions of the GI system. The drug loading procedure would be carried out in the step when Carbopol and cellulose acetate powdered forms are pill-pressed into a thin tablet. For a uniform distribution of the drug loaded onto the


**Figure 3-11.** A model of the Janus device.

device, the chosen drug can be mixed into a homogeneous solution with cellulose acetate and solvent, and then that solution can be reprecipitated back into the powdered form to be pill-pressed with the Carbopol layer. Moreover, the designed protocol also does not require expensive equipment, complicated chemical procedure, or long fabrication time.

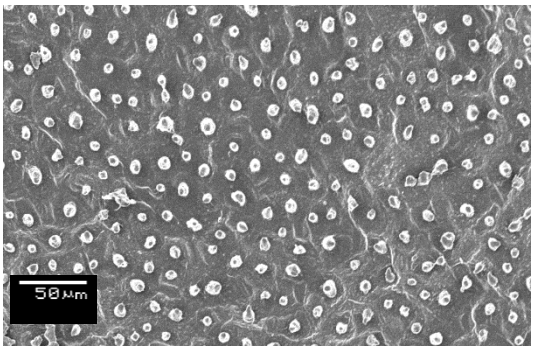


**Figure 3-12.** SEM image of the nanoposts on the cellulose acetate side of the fabricated Janus device following the drafted protocol.

To test and demonstrate the compatibility of designed protocol with our proposed system, the finished Janus product was characterized by SEM. As seen in Figure 3-12, the SEM image of the modified cellulose acetate surface showed signs of surface roughening with the creation of the nano-structures, similar to those on the lotus leaf. The SEM analysis confirmed that that the nanoposts were successfully replicated from the lotus leaf imprint onto the cellulose acetate side of the fabricated dual layer through our designed protocol. Also, simple touch tests verified that the Carbopol side demonstrated strong mucoadhesion when wetted. Therefore, overall, the designed protocol is shown to be feasible, reproducible, low-cost, and efficient in its fabrication process. It also fulfills its purpose of delivering drug to the site of administration, as it allows for a controllable and extended release of the drug.

### 3.6 *In Vitro* Studies

As outlined in section *2.6*, *in vitro* macroscopic evaluation was carried out by placing a Janus device (omniphobic and adhesive) and a non-Janus device (adhesive on both side) on a piece of porcine small intestinal tissue and pumping a stream of water over the tissue. Note

that esophageal tissue was not initially used because it was not available in time for these *in vitro* experiments. Future work will involve repeating this macroscopic evaluation using porcine esophageal tissues as well as other GI tissues. The time-lapse photography, shown in Figure 3-13, was collected from the video recording of one of the three conducted trials. All three trials demonstrated the same behavior and effect.

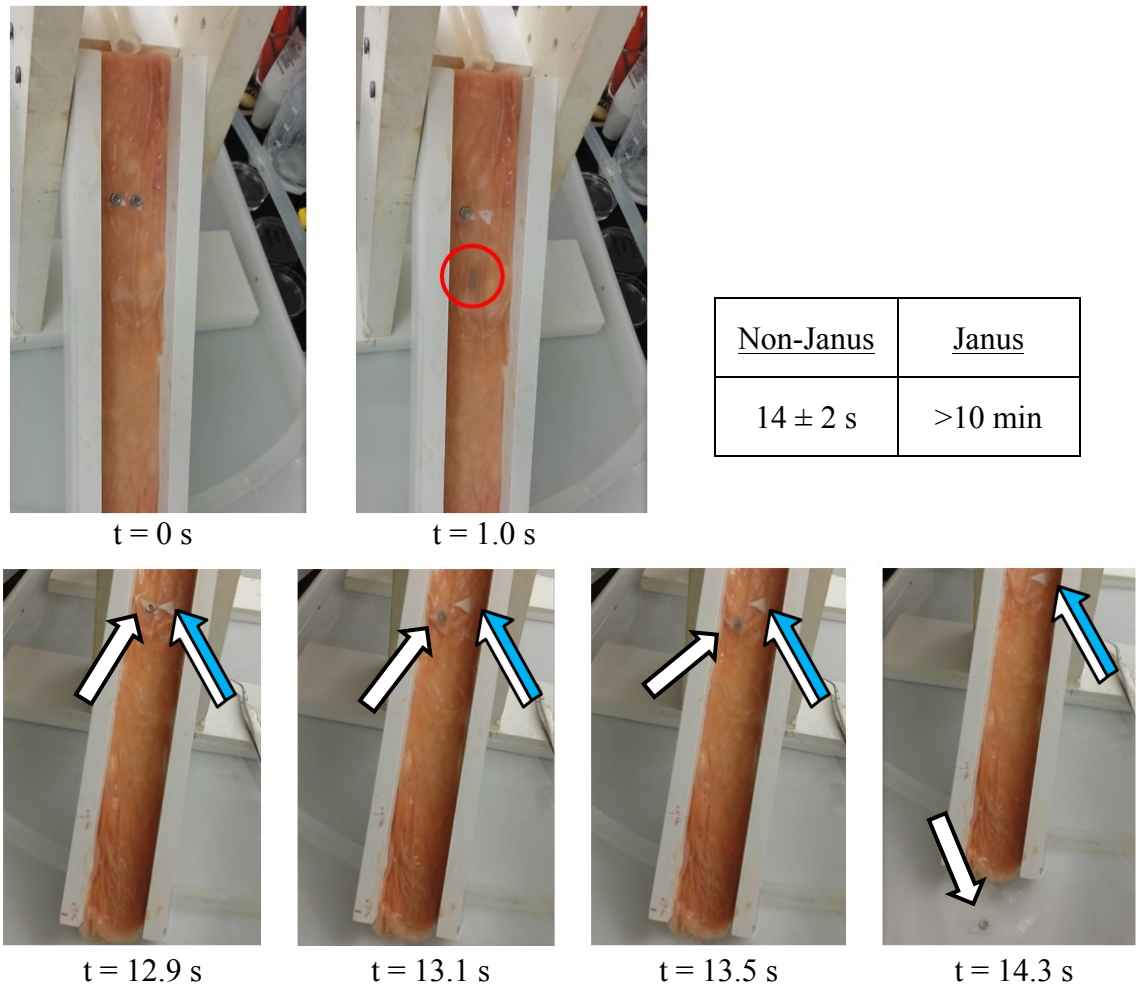


| Non-Janus | Janus |
|---|---|
| 14 ± 2 s | >10 min |

**Figure 3-13.** A time-lapse photography collected from the video recording of one of the *in vitro* trials. The sample on the left represents the non-Janus device, while the sample on the right represents the Janus device. The red circle indicates the dislodgement of the weight from the omniphobic side of the Janus device. The series of the white arrows traces the dislodgement of the non-Janus device (one with the weight not detached). The series of the dual-colored arrows traces the retention of the Janus device (one with the weight detached). The mean values and standard deviations of the retention times are reported (n = 3).

In the time-lapse photography shown in Figure 3-13, the distinction between the Janus device (right) and the non-Janus device (left) could be made by observing the dislodgement

of the weight purportedly placed on top of each device. On the Janus device with the omniphobic side facing out, the weight would fall off the omniphobic side instantly, for the omniphobicity of the surface minimizes any undesirable interactions with the surface and foreign objects. On the other hand, on the non-Janus device with the adhesive side facing out, the weight would remain stuck on the adherent side. The weight was used to speed up the dislodgement of the devices in order to observe the effect in an accelerated time frame. It also represented the aggregation with the foodstuffs expected when the device is attached to the GI mucosal wall. The Janus device was retained on the tissue for a longer period of time than the non-Janus device, shown in Figure 3-13. Over the three trials, while the non-Janus device became dislodged after 14 ± 2 seconds, the Janus device remained stuck on the tissue for more than 10 minutes, at which time the measurements were stopped. We could conclude that this effect was seen mainly because the weight stuck on the non-Janus device created more interaction with the water flowing down the tissue; as the friction between the device and the flowing water increased, more force was exerted to bring down the device.

The results illustrated the purpose of incorporating omniphobicity in our system design of the Janus device (sketched in section *1.6*). This omniphobic side would prevent aggregation with the foodstuffs on the device when attached onto the GI mucosal wall and thus avoid easy detachment. Therefore, these *in vitro* studies confirmed our expected behavior of the Janus device, which demonstrated longer retention in comparison to the non-Janus device. In other words, these studies showed that our drug-delivery system was designed to effectively minimize the interaction with foodstuffs and reduce the likelihood of dislodgement, which can be attributed to the incorporation of omniphobicity.

# 4. CONCLUSION

A drug-delivery device with the unique capacity for extended GI retention and drug release was successfully developed by fabricating a novel Janus device that is low-cost, self-healing, and durable. A flat dual layer was fabricated, in which one side is mucoadhesive, enabling adhesion to the GI mucosa, and the other side is omniphobic, repelling foodstuffs and bodily secretions traveling rapidly down the esophagus. This design with the polymer located between the two layers allows tunable loading capacity, including adjustable amount of drug loaded, controllable release of the desired drug, and protection of the drug from acidic conditions of the GI system.

For the omniphobic side, the surface was first successfully modified by soft lithography to carry out morphological replication of the micro-structures or nanoposts on the superhydrophobic lotus leaves. The high quality of the replication was verified by SEM. Then, through chemical modification mediated by fluorination and lubrication, we were able to achieve omniphobicity on the surface. For the mucoadhesive side, mussel-inspired surface chemistry using dopamine was initially attempted, but we could not achieve the desired mucoadhesion on the surface. Therefore, we used an alternative mucoadhesive polymer, Carbopol, which demonstrated strong mucoadhesion when wetted. For future applications, different approaches involving chemical functionalization of various mucoadhesive ligands on platform polymers to attain mucoadhesion will be investigated. Omniphobicity or mucoadhesion of a side was characterized and verified using contact angle goniometry. The protocol for creating the desired Janus device was designed and carried out successfully. *In vitro* studies using porcine tissues manifested that the dual-sided nature of the Janus device allowed for extended retention on the GI mucosal wall.

Future work will include conducting Franz diffusion cell tests, in which we will show the effect of omniphobicity in facilitating unidirectional drug delivery. Through these diffusion tests, we would like to demonstrate that the drug would be released through the mucoadhesive side, directly to the targeted region of the mucosa, and be impermeable through the omniphobic side. Unidirectional drug release would give us a highly efficient drug-delivery system, in which drug loss and undesirable side effects are minimized. Additionally, *in vivo* studies will be carried out to assess extended retention and drug release. The stability and degradation of the fabricated Janus devices in the acidic environment of the GI tract will also be investigated. This would involve feeding fluorescently labeled devices to rodent models and monitoring the retention of the devices. The rats will ingest a number of devices, in which half of them will be Janus devices with adhesive and omniphobic sides and the other half will be non-Janus devices that are either completely adhesive or omniphobic. The retention extent will be compared between the devices by quantifying the level of fluorescence inside the rats' GI tract. Ultimately, with successful fabrication and validation, this engineered Janus device will have promising biomedical applications with the potential to improve treatment for diseases of the GI tract.

# 5. REFERENCES


1. Osterberg, L.; Blaschke, T., Adherence to medication. *N Engl J Med* **2005,** *353* (5), 487-97.
2. Sabaté, E.; Organization, W. H., *Adherence to Long-term Therapies: Evidence for Action*. World Health Organization: 2003.
3. Benner, J. S.; Glynn, R. J.; Mogun, H.; Neumann, P. J.; Weinstein, M. C.; Avorn, J., LOng-term persistence in use of statin therapy in elderly patients. *JAMA : the journal of the American Medical Association* **2002,** *288* (4), 455-461.
4. Shaji, J.; Patole, V., Protein and Peptide drug delivery: oral approaches. *Indian J Pharm Sci* **2008,** *70* (3), 269-77.
5. Pinto, J. F., Site-specific drug delivery systems within the gastro-intestinal tract: From the mouth to the colon. *Int. J. Pharm.* **2010,** *395* (1–2), 44-52.
6. Fischer, W.; Boertz, A.; Davis, S. S.; Khosla, R.; Cawello, W.; Sandrock, K.; Cordes, G., Investigation of the gastrointestinal transit and in vivo drug release of isosorbide-5-nitrate pellets. *Pharm. Res.* **1987,** *4* (6), 480-5.
7. Chen, J.; Blevins, W. E.; Park, H.; Park, K., Gastric retention properties of superporous hydrogel composites. *J. Controlled Release* **2000,** *64* (1–3), 39-51.
8. Walther, A.; Müller, A. H. E., Janus Particles: Synthesis, Self-Assembly, Physical Properties, and Applications. *Chem. Rev.* **2013,** *113* (7), 5194-5261.
9. Casagrande, C.; Veyssié, M., 'Grains Janus': Réalisation et premières observations des propriétés interfaciales. *C. R. Acad. Sci. (Paris)* **1988,** *306*, 1423.
10. de Gennes, P.-G., Soft Matter (Nobel Lecture). *Angewandte Chemie International Edition in English* **1992,** *31* (7), 842-845.
11. Kaewsaneha, C.; Tangboriboonrat, P.; Polpanich, D.; Eissa, M.; Elaissari, A., Janus colloidal particles: preparation, properties, and biomedical applications. *ACS Appl Mater Interfaces* **2013,** *5* (6), 1857-69.
12. Hwang, S.; Lahann, J., Differentially Degradable Janus Particles for Controlled Release Applications. *Macromol. Rapid Commun.* **2012,** *33* (14), 1178-1183.
13. Choi, J. S.; Jun, Y. W.; Yeon, S. I.; Kim, H. C.; Shin, J. S.; Cheon, J., Biocompatible heterostructured nanoparticles for multimodal biological detection. *J. Am. Chem. Soc.* **2006,** *128* (50), 15982-3.
14. Hu, S. H.; Gao, X., Nanocomposites with spatially separated functionalities for combined imaging and magnetolytic therapy. *J. Am. Chem. Soc.* **2010,** *132* (21), 7234-7.
15. Shaikh, R.; Raj Singh, T. R.; Garland, M. J.; Woolfson, A. D.; Donnelly, R. F., Mucoadhesive drug delivery systems. *J Pharm Bioallied Sci* **2011,** *3* (1), 89-100.
16. Boddupalli, B. M.; Mohammed, Z. N. K.; Nath, R. A.; Banji, D., *Mucoadhesive drug delivery system: An overview*. 2010; Vol. 1, p 381-7.
17. Ahuja, A.; Khar, R. K.; Ali, J., Mucoadhesive Drug Delivery Systems. *Drug Dev. Ind. Pharm.* **1997,** *23* (5), 489-515.
18. Jiménez-castellanos, M. R.; Zia, H.; Rhodes, C. T., Mucoadhesive Drug Delivery Systems. *Drug Dev. Ind. Pharm.* **1993,** *19* (1-2), 143-194.
19. Ch'ng, H. S.; Park, H.; Kelly, P.; Robinson, J. R., Bioadhesive polymers as platforms for oral controlled drug delivery II: synthesis and evaluation of some swelling, water-insoluble bioadhesive polymers. *J. Pharm. Sci.* **1985,** *74* (4), 399-405.
20. Kremser, C.; Albrecht, K.; Greindl, M.; Wolf, C.; Debbage, P.; Bernkop-Schnurch, A., In vivo determination of the time and location of mucoadhesive drug delivery systems disintegration in the gastrointestinal tract. *Magn Reson Imaging* **2008,** *26* (5), 638-43.
21. Albrecht, K.; Greindl, M.; Kremser, C.; Wolf, C.; Debbage, P.; Bernkop-Schnurch, A., Comparative in vivo mucoadhesion studies of thiomer formulations using magnetic resonance imaging and fluorescence detection. *J Control Release* **2006,** *115* (1), 78-84.
22. Zaghloul, A.; Taha, E.; Afouna, M.; Khattab, I.; Nazzal, S., Ex vivo mucoadhesion and in vivo bioavailability assessment and correlation of ketoprofen tablet dosage forms containing bioadhesives. *Pharmazie* **2007,** *62* (5), 346-50.
23. Ahmed, I. S.; Ayres, J. W., Bioavailability of riboflavin from a gastric retention formulation. *Int. J. Pharm.* **2007,** *330* (1-2), 146-54.
24. Salman, H. H.; Gamazo, C.; Agueros, M.; Irache, J. M., Bioadhesive capacity and immunoadjuvant properties of thiamine-coated nanoparticles. *Vaccine* **2007,** *25* (48), 8123-32.

25. Khutoryanskiy, V. V., Advances in Mucoadhesion and Mucoadhesive Polymers. *Macromolecular Bioscience* **2011,** *11* (6), 748-764.
26. Lee, H.; Dellatore, S. M.; Miller, W. M.; Messersmith, P. B., Mussel-inspired surface chemistry for multifunctional coatings. *Science (New York, N.Y.)* **2007,** *318* (5849), 426-30.
27. Chen, G.; Xia, Y.; Lu, X.; Zhou, X.; Zhang, F.; Gu, N., Effects of surface functionalization of PLGA membranes for guided bone regeneration on proliferation and behavior of osteoblasts. *Journal of biomedical materials research. Part A* **2013,** *101* (1), 44-53.
28. Yang, K.; Lee, J. S.; Kim, J.; Lee, Y. B.; Shin, H.; Um, S. H.; Kim, J. B.; Park, K. I.; Lee, H.; Cho, S. W., Polydopamine-mediated surface modification of scaffold materials for human neural stem cell engineering. *Biomaterials* **2012,** *33* (29), 6952-64.
29. Schäfer-Korting, M., *Drug Delivery*. Springer-Verlag: 2010.
30. Wong, T. S.; Kang, S. H.; Tang, S. K.; Smythe, E. J.; Hatton, B. D.; Grinthal, A.; Aizenberg, J., Bioinspired self-repairing slippery surfaces with pressure-stable omniphobicity. *Nature* **2011,** *477* (7365), 443-7.
31. Vogel, N.; Belisle, R. A.; Hatton, B.; Wong, T. S.; Aizenberg, J., Transparency and damage tolerance of patternable omniphobic lubricated surfaces based on inverse colloidal monolayers. *Nat Commun* **2013,** *4*, 2167.
32. Nosonovsky, M.; Bhushan, B., Superhydrophobic surfaces and emerging applications: Non-adhesion, energy, green engineering. *Current Opinion in Colloid & Interface Science* **2009,** *14* (4), 270-280.
33. Barthlott, W.; Neinhuis, C., Purity of the sacred lotus, or escape from contamination in biological surfaces. *Planta* **1997,** *202* (1), 1-8.
34. Michael, N., Materials science: Slippery when wetted. *Nature* **2011,** *477* (7365), 412-413.
35. Cassie, A. B. D.; Baxter, S., Wettability of porous surfaces. *Transactions of the Faraday Society* **1944,** *40* (0), 546-551.
36. Akira, N., Design of hydrophobic surfaces for liquid droplet control. *NPG Asia Materials* **2011,** *3* (5), 49-56.
37. Webb, H. K.; Crawford, R. J.; Ivanova, E. P., Wettability of natural superhydrophobic surfaces. *Adv. Colloid Interface Sci.* (0).
38. Batchelor, H., Bioadhesive dosage forms for esophageal drug delivery. *Pharm. Res.* **2005,** *22* (2), 175-81.
39. Li, Q.; Castell, J. A.; Castell, D. O., Manometric determination of esophageal length. *Am J Gastroenterol* **1994,** *89* (5), 722-5.
40. Cordova-Fraga, T.; Sosa, M.; Wiechers, C.; De la Roca-Chiapas, J. M.; Maldonado Moreles, A.; Bernal-Alvarado, J.; Huerta-Franco, R., Effects of anatomical position on esophageal transit time: a biomagnetic diagnostic technique. *World J Gastroenterol* **2008,** *14* (37), 5707-11.
41. Zhang, L.; Russell, D.; Conway, B. R.; Batchelor, H., Strategies and therapeutic opportunities for the delivery of drugs to the esophagus. *Crit Rev Ther Drug Carrier Syst* **2008,** *25* (3), 259-304.
42. Hommel, K. A.; Franciosi, J. P.; Hente, E. A.; Ahrens, A.; Rothenberg, M. E., Treatment adherence in pediatric eosinophilic gastrointestinal disorders. *J Pediatr Psychol* **2012,** *37* (5), 533-42.
43. Guilloteau, P.; Zabielski, R.; Hammon, H. M.; Metges, C. C., Nutritional programming of gastrointestinal tract development. Is the pig a good model for man? *Nutr Res Rev* **2010,** *23* (1), 4-22.
44. Li, H.; Yu, Q.; Chen, L.; Chen, M., Polymer composites and fabrications thereof. Google Patents: 2012.
45. Lepore, E.; Pugno, N., Superhydrophobic Polystyrene by Direct Copy of a Lotus Leaf. *BioNanoSci.* **2011,** *1* (4), 136-143.
46. Croll, T. I.; O'Connor, A. J.; Stevens, G. W.; Cooper-White, J. J., Controllable surface modification of poly(lactic-co-glycolic acid) (PLGA) by hydrolysis or aminolysis I: physical, chemical, and theoretical aspects. *Biomacromolecules* **2004,** *5* (2), 463-73.
47. Xu, J.; Soliman, G. M.; Barralet, J.; Cerruti, M., Mollusk glue inspired mucoadhesives for biomedical applications. *Langmuir : the ACS journal of surfaces and colloids* **2012,** *28* (39), 14010-7.
48. Xiong, X.; Qu, S.-x.; Liu, Y.-m., Synthesis and characterization of Dopamine graft compound N-methacryloyl 3,4-dihydroxyl-phenylamine. *Journal of Physics: Conference Series* **2013,** *419* (1), 012047.
49. Suffern, D.; Clarke, S. J.; Hollmann, C. A.; Bahcheli, D.; Bradforth, S. E.; Nadeau, J. L. In *Labeling of subcellular redox potential with dopamine-conjugated quantum dots*, 2006; pp 60960O-60960O-12.
50. Lane, C. F., Sodium Cyanoborohydride - A Highly Selective Reducing Agent for Organic Functional Groups. *Synthesis* **1975,** *1975* (03), 135-146.
51. Sun, C. J.; Srivastava, A.; Reifert, J. R.; Waite, J. H., Halogenated DOPA in a Marine Adhesive Protein. *J. Adhes.* **2009,** *85* (2-3), 126.